Intermodal four-wave mixing in a higher-order-mode fiber

Ji Cheng,[1,a)] Martin E. V. Pedersen,[2,a)] Kriti Charan,[1] Ke Wang,[1] Chris Xu,[1,b)] Lars Grüner-Nielsen,[2] and Dan Jakobsen[2]
[1]*School of Applied and Engineering Physics, Cornell University, Ithaca, New York 14853, USA*
[2]*OFS Fitel Denmark, Priorparken 680, 2605 Brondby, Denmark*

(Received 18 June 2012; accepted 1 October 2012; published online 16 October 2012)

We demonstrate a high-efficiency intermodal four-wave-mixing process in an all-fiber system, comprising a picosecond fiber laser and a high-order-mode (HOM) fiber. Two pump photons in the LP_{01} mode of the fiber can generate an anti-Stokes photon in the LP_{01} mode and a Stokes photon in the LP_{02} mode. The wavelength dependent mode profiles of the HOM fiber produce significant spatial overlap between the modes involved. The anti-Stokes wave at 941 nm is generated with 20% conversion efficiency with input pulse energy of 20 nJ. The guidance of the anti-Stokes and Stokes waves in the HOM fiber enhances system stability. © *2012 American Institute of Physics*. [http://dx.doi.org/10.1063/1.4759038]

Four-wave mixing (FWM) in optical fibers has been utilized for nonlinear frequency conversion. FWM has been studied in single-mode fibers, multimode fibers, and more recently, photonic crystal fibers (PCFs).[1–8] In most experiments, the red-shifted Stokes wave and the blue-shifted anti-Stokes wave are generated within the same mode as the pump light. In these cases, the phase-matching conditions require the pump to be in the vicinity of the zero dispersion wavelength (ZDW) of the propagating mode.[8,9] However, launching high power pump light near the ZDW can easily generate a supercontinuum (SC), which limits the conversion efficiency from the pump to the narrow-band Stokes and anti-Stokes waves.[10] High-efficiency FWM generation at 673 nm and 2539 nm has been achieved in an endlessly single-mode large-mode-area (LMA) PCF without having the pump light close to the ZDW.[11] However, this approach cannot be extended to generate light at other wavelengths, since the phase-matching condition is predominantly defined by the material dispersion. To overcome the limitation of FWM within a single spatial mode, an intermodal FWM approach has been proposed.[12] In this approach, pump light is launched in the normal dispersion region of the fundamental mode. The Stokes and the anti-Stokes waves can satisfy the phase-matching condition by propagating in other higher-order-modes (HOMs). This effect has been observed in conventional and Ge-doped multimode fibers at visible wavelengths, using a high power pump at 532 nm.[3,4] Recently, the effect has been studied more systematically in PCFs.[12–14]

Intermodal FWM has several advantages over traditional single-mode FWM. This method can achieve high conversion efficiency without SC generation.[12] The wavelength of the Stokes and anti-Stokes light can be easily controlled by fiber design, such as changing the core diameter.[4,13] More importantly, intermodal FWM provides extra degrees of freedom, thus increased flexibility, in fiber designs to generate FWM, because the phase-matching condition can be fulfilled with more than one propagating mode. However, intermodal FWM demonstrations so far require a high-power laser source, such as a Q-switched Nd:YAG laser or a Ti:Sapphire regenerative amplifier. As a result, they are typically used to generate light with high pulse energy ($\sim\mu$J) and low repetition rate ($\sim$100 kHz). In addition, the HOMs are only weakly guided in PCFs; therefore, the efficiency of intermodal FWM can be extremely sensitive to perturbations of the fiber. The combination of a high power pump source and PCFs also makes the system difficult to integrate into an all-fiber configuration. In this Letter, we demonstrate efficient intermodal FWM in an all-fiber system that consists of a picosecond passive mode-locked fiber laser and a HOM fiber. Compared with previous experiments, intermodal FWM in the HOM fiber requires much lower input pulse energy ($\sim$20 nJ) and provides much improved stability. The phase-matching condition is fulfilled between two pump photons at 1064 nm in the LP_{01} mode, one anti-Stokes photon in the LP_{01} mode, and one Stokes photon in the LP_{02} mode. The anti-Stokes and Stokes waves are generated, respectively, at 941 nm and 1225 nm, each with 20% conversion efficiency. Both waves are well-guided in the HOM fiber, and the large effective refractive index (n_{eff}) difference between the modes suppresses mode coupling. Due to these characteristics, intermodal FWM in the HOM fiber has much better stability than in the PCFs. Intermodal FWM is potentially another valuable application for HOM fibers, which have been used primarily for dispersion compensation, soliton generation, and signal transmission.[15–17]

The all-fiber system uses a homemade fiber laser to provide input pulses to the HOM fiber. The mode-locked fiber laser consists of a seed oscillator at 1064 nm and two ytterbium doped fiber amplifiers. The output of the fiber laser is an 18.33 MHz pulse train with a maximal power of 470 mW. The pulse width is approximately 6 ps. The fiber laser is directly spliced to 1.75 m of HOM fiber, using a core alignment fusion splicer (Fujikura FSM-30S Splicer). After the fiber splice, more than 95% of the power in the HOM fiber is guided in the LP_{01} mode. An optical spectrum analyzer and a second-order autocorrelator are used to characterize the spectral and temporal features of the Stokes and anti-Stokes pulses. The spatial profiles of the two pulses are magnified

[a)]Ji Cheng and Martin E. V. Pedersen contributed equally to this work.
[b)]Author to whom correspondence should be addressed. Electronic mail: cx10@cornell.edu.

 © 2012 American Institute of Physics

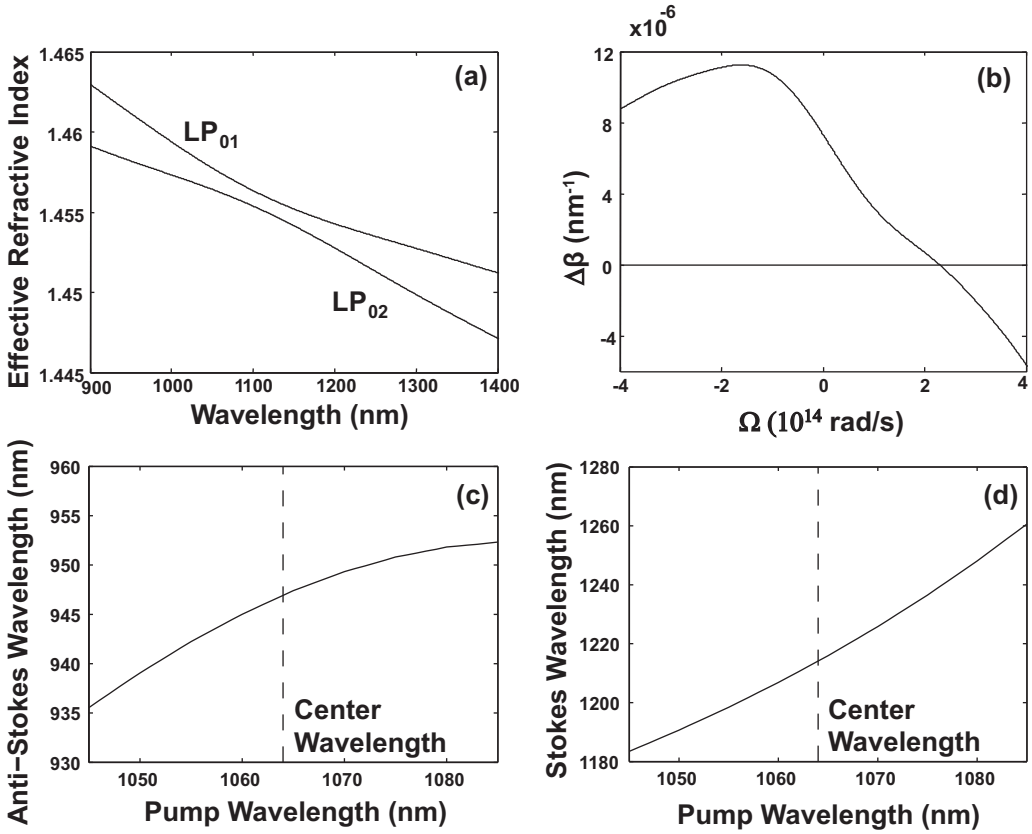

FIG. 1. (a) Calculated effective refractive indices of the LP_{01} (solid) and the LP_{02} (dashed) modes. (b) Propagation constant mismatch, $\Delta\beta$, as a function of Stokes shift Ω, for pump wavelength at 1064 nm. The dashed line indicates the phase matching condition. Calculated anti-Stokes wavelength (c) and Stokes wavelength (d) as functions of the pump wavelength. The dashed line indicates the center pump wavelength.

by a factor of 100 in a 4f system and are measured by scanning a 20-μm pinhole together with a germanium photodiode detector. The HOM fiber is designed to have large normal and anomalous dispersion at 1064 nm in the LP_{01} and the LP_{02} modes, respectively. The calculated effective refractive indices for the LP_{01} and the LP_{02} modes of the HOM fiber are shown in Fig. 1(a). The dispersion and group delay derived from the effective refractive indices are in good agreement with experimental measurements.[18] At the pump wavelength of 1064 nm, the LP_{01} mode of the HOM fiber has large normal dispersion, which effectively suppresses SC generation.

To generate a Stokes photon in the LP_{02} mode and an anti-Stokes photon in the LP_{01} mode, the mismatch of the propagation constant, $\Delta\beta$, which can be written as $2\beta_{01,P} - \beta_{01,A}(\Omega) - \beta_{02,S}(\Omega)$, must be zero (i.e., phase matching condition).[9] Here, β is the propagation constant, and the subscripts represent the pump (P), anti-Stokes (A), and Stokes (S) in the LP_{01} mode (01) and the LP_{02} mode (02). Ω is the Stokes shift. $\Delta\beta$ as a function of Ω can be calculated from the effective refractive indices and is shown in Fig. 1(b). In the HOM fiber, we can neglect the nonlinear contribution from the pump light to the phase matching condition when the peak power is below 10 kW. When pumped at 1064 nm, the phase-matching condition is satisfied at $\Omega = 2.3 \times 10^{14}$ rad/s, corresponding to a Stokes wavelength of 1225 nm and an anti-Stokes wavelength of 941 nm. The calculated anti-Stokes and Stokes wavelengths at different pump wavelengths are shown in Figs. 1(c) and 1(d). Note that the anti-Stokes wavelength is much less sensitive to the pump wavelength, which is similar to the results for intermodal FWM in PCFs.[12]

The theoretical prediction of intermodal FWM is validated by our experimental results. Fig. 2 shows the measured spectra at the output of the HOM fiber at various input pulse energies. For pump powers below 200 mW (11 nJ input energy), only self-phase modulation induced spectral broadening can be observed. As the input power increases, the

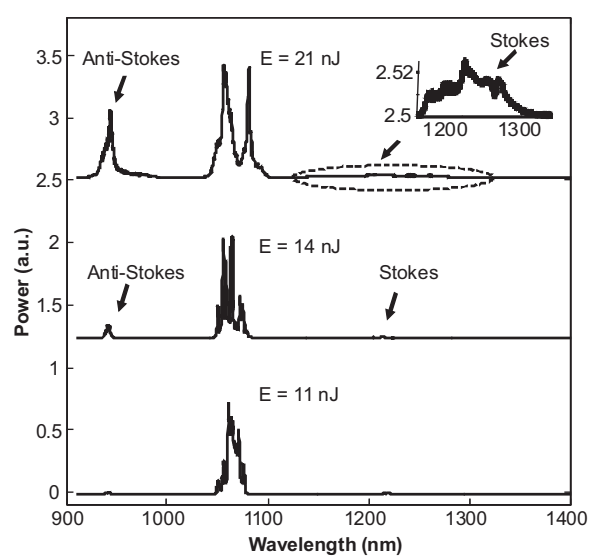

FIG. 2. Output spectra after 1.75 m of HOM fiber with input pulse energies of 11, 14, and 21 nJ. Inset: Spectrum of the Stokes light at input energy of 21 nJ.

pump spectrum degrades due to the high nonlinearity. At 250 mW (14 nJ pulse energy) of pump power, strong, narrowband anti-Stokes light at 941 nm and broadband Stokes light at 1225 nm are simultaneously generated through intermodal FWM. The center wavelengths of both sidebands accurately match our calculation. The bandwidth of the anti-Stokes light is much narrower than that of the Stokes light since the anti-Stokes' wavelength is much less sensitive to the pump wavelength than the Stokes' wavelength is. This yields a much higher spectral power density in the anti-Stokes light.

Measured spatial profiles (magnified by 100×) of the anti-Stokes and Stokes light, shown in Figs. 3(a) and 3(b), indicate that they propagate in the LP_{01} and the LP_{02} modes, respectively.[19] These measurement results are in good agreement with the calculated spatial profiles of the LP_{01} mode at 940 nm and the LP_{02} mode at 1225 nm. The measured profiles show that both waves are tightly confined in the core with a radius smaller than 2 μm. In a triple clad HOM fiber, the LP_{02} mode monotonically transitions to the higher-index core from the lower-index ring of the fiber, as the wavelength increases.[15] Consequently, the LP_{02} mode at the Stokes wavelength is very concentrated with approximately 80% of the power in the core and overlaps significantly with the LP_{01} mode at the anti-Stokes and pump wavelengths. The effective area that represents the spatial overlap of this intermodal FWM process can be written as

$$\left[\int\int_{-\infty}^{\infty} F_{01,P}(x,y).F^{*}_{01,P}(x,y).F_{01,A}(x,y).F^{*}_{02,S}(x,y).dxdy\right]^{-1}, \tag{1}$$

where $F_{01,P}(x, y)$, $F_{01,A}(x, y)$, and $F_{02,S}(x, y)$ are the normalized mode profiles of the pump, anti-Stokes, and Stokes wave, respectively (see derivations from Ref. 4). Based on the spatial distributions of the LP_{01} and the LP_{02} modes of the HOM fiber, we obtain a relatively small effective area of approximately 7 μm^2. This small effective area for the intermodal FWM process enables a strong intermodal nonlinear interaction at relatively low input peak power. Hence, spontaneous intermodal FWM can be generated in this HOM fiber at a peak power of just 2 kW, which is 3 orders of magnitude smaller than the peak power required in LMA PCFs at a comparable wavelength. The strong intermodal nonlinearity also ensures a high efficiency for wavelength conversion. With 385 mW (21 nJ pulse energy) coupled into the HOM fiber, approximately 78 mW (4.2 nJ pulse energy) is generated in the anti-Stokes sideband, corresponding to 20% power conversion efficiency. The anti-Stokes pulse has a spectral full width at half maximum (FWHM) of 10 nm (Fig. 2), corresponding to 8 mW/nm spectral power density.

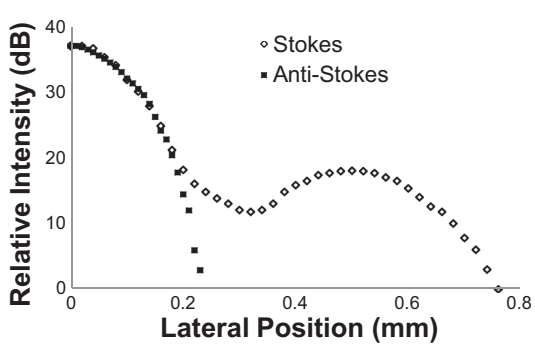

FIG. 3. Measured spatial profiles of the anti-Stokes light at 941 nm and the Stokes light at 1225 nm, magnified by a factor of 100. Note that the vertical axes are in logarithmic scale. (Adapted from Ref. 19. Copyright 2012, The Optical Society.)

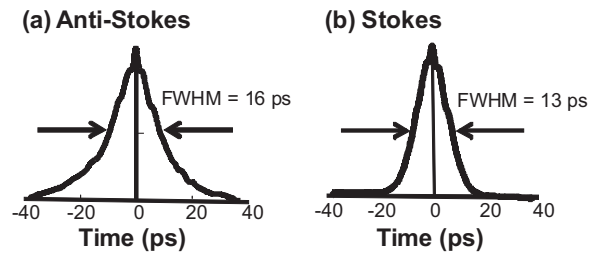

FIG. 4. Measured second-order intensity autocorrelation traces of the anti-Stokes pulse (a) and Stokes pulse (b) at input pulse energy of 21 nJ. (Adapted from Ref. 19. Copyright 2012, The Optical Society.)

The group index of the pump light in the LP_{01} mode, the anti-Stokes light in the LP_{01} mode, and the Stokes light in the LP_{02} mode are respectively 1.494, 1.488, and 1.487. Due to the group velocity difference, there is significant temporal walk-off between the pump and the anti-Stokes and Stokes pulses generated from the FWM process, which was also observed in previous work.[20] Based on the group index and the input pulse width, the walk-off length of the FWM process is 30 cm, much longer than the nonlinear length (i.e., 2 cm at 14 nJ input energy), and thus, the efficiency of FWM is not significantly affected.[21] However, the anti-Stokes and Stokes pulses are significantly broadened temporally due to both the temporal walk-off and the group velocity dispersion. The second-order intensity autocorrelation of the anti-Stokes and Stokes light at input pulse energy of 21 nJ are measured and shown in Figs. 4(a) and 4(b), respectively.[19] The FWHMs of intensity autocorrelation trace of the anti-Stokes and Stokes pulses are 16 and 13 ps, respectively. The autocorrelation measurement also shows good stability of the anti-Stokes and Stokes pulses. Because both the LP_{01} and the LP_{02} modes are well-guided in the HOM fibers, the demonstrated intermodal FWM effect is much less sensitive to fiber perturbations than in PCFs, where the anti-Stokes and Stokes bands generated by the intermodal FWM can be significantly attenuated by bending the fiber.[12]

In conclusion, we demonstrate intermodal FWM in a HOM fiber. The all-fiber system based on the HOM fiber can efficiently generate anti-Stokes and Stokes pulses at a low input peak power of 2 kW. Intermodal FWM in the HOM fiber also has better stability than similar phenomena reported in PCFs. Intermodal FWM in a HOM fiber provides a fiber platform for simultaneous, nonlinear wavelength conversion, and mode conversion. This fiber platform can be tailored to other wavelengths of interest, such as the 1550 nm spectral window for fiber optic communications. The phenomenon reported here could affect performance by introducing cross-talks in mode division multiplexing transmission systems.[17] However, intermodal FWM may potentially find applications in mode and wavelength conversion.

The research was supported in part by NIH R01CA133148 and R21RR024415. The authors thank Frank Wise for sharing equipment.

[1]K. O. Hill, D. C. Johnson, B. S. Kawasaki, and R. I. MacDonald, J. Appl. Phys. **49**, 5098–5106 (1978).
[2]K. Inoue and H. Toba, IEEE Photon. Technol. Lett. **4**, 69–72 (1992).
[3]R. H. Stolen, J. E. Bjorkholm, and A. Ashkin, Appl. Phys. Lett. **24**, 308–310 (1974).
[4]C. Lin and M. A. Bösch, Appl. Phys. Lett. **38**, 479–481 (1981).
[5]J. E. Sharping, Y. Okawachi, J. van Howe, C. Xu, Y. Wang, A. E. Willner, and A. L. Gaeta, Opt. Express **13**, 7872–7877 (2005).
[6]C. J. McKinstrie, S. Radic, and A. R. Chraplyvy, IEEE J. Sel. Top. Quantum Electron. **8**, 538–547 (2002).
[7]J. E. Sharping, M. Fiorentino, A. Coker, P. Kumar, and R. S. Windeler, Opt. Lett. **26**, 1048–1050 (2001).
[8]W. J. Wadsworth, N. Joly, J. C. Knight, T. A. Birks, F. Biancalana, and P. St. J. Russell, Opt. Express **12**, 299–309 (2004).
[9]G. P. Agrawal, *Nonlinear Fiber Optics*, 4th ed. (Academic Press, Boston, 2007).
[10]J. M. Dudley, G. Genty, and S. Coen, Rev. Mod. Phys. **78**, 1135–1184 (2006).
[11]D. Nodop, C. Jauregui, D. Schimpf, J. Limpert, and A. Tünnermann, Opt. Lett. **34**, 3499–3501 (2009).
[12]H. Tu, Z. Jiang, D. L. Marks, and S. A. Boppart, Appl. Phys. Lett. **94**, 101109 (2009).
[13]A. Labruyere, A. Martin, P. Leproux, V. Couderc, A. Tonello, and N. Traynor, Opt. Express **16**, 21997–22002 (2008).
[14]C. Lesvigne, V. Couderc, A. Tonello, P. Leproux, A. Barthélémy, S. Lacroix, F. Druon, P. Blandin, M. Hanna, and P. Georges, Opt. Lett. **32**, 2173–2175 (2007).
[15]S. Ramachandran, S. Ghalmi, J. W. Nicholson, M. F. Yan, P. Wisk, E. Monberg, and F. V. Dimarcello, Opt. Lett. **31**, 2532–2534 (2006).
[16]J. van Howe, J. H. Lee, S. Zhou, F. Wise, C. Xu, S. Ramachandran, S. Ghalmi, and M. F. Yan, Opt. Lett. **32**, 340–342 (2007).
[17]S. Randel, R. Ryf, A. Sierra, P. J. Winzer, A. H. Gnauck, C. A. Bolle, R. Essiambre, D. W. Peckham, A. McCurdy, and R. Lingle, Opt. Express **19**, 16697–16707 (2011).
[18]J. Cheng, M. E. V. Pedersen, K. Wang, C. Xu, L. Grüner-Nielsen, and D. Jakobsen, Opt. Lett. **37**, 347–349 (2012).
[19]J. Cheng, M. E. V. Pedersen, K. Charan, C. Xu, L. Grüner-Nielsen, and D. Jakobsen, in *Conference on Lasers and Electro-Optics (CLEO)*, San Jose, California, May 2012, p. CTh3G.6.
[20]Y. Q. Xu, S. G. Murdoch, R. Leonhardt, and J. D. Harvey, Opt. Lett. **33**, 1351–1353 (2008).
[21]F. Poletti and P. Horak, Opt. Express **17**, 6134–6147 (2009).